HHS Public Access

Author manuscript

Nat Neurosci. Author manuscript; available in PMC 2016 March 01.

Published in final edited form as:

Nat Neurosci. 2015 September ; 18(9): 1299–1309. doi:10.1038/nn.4082.

Dynamic Re-wiring of Neural Circuits in the Motor Cortex in Mouse Models of Parkinson's Disease

Lili Guo[#1,2], **Huan Xiong**[#1,2], **Jae-Ick Kim**[#3,4,5], **Yu-Wei Wu**[#3,4,5], **Rupa R. Lalchandani**[3,4,5], **Yuting Cui**[1,2], **Yu Shu**[1,2], **Tonghui Xu**[1,2], and **Jun B. Ding**[3,4,5]

[1]Britton Chance Center for Biomedical Photonics, Wuhan National Laboratory for Optoelectronics-Huazhong University of Science and Technology, Wuhan 430074, China

[2]MoE Key Laboratory for Biomedical Photonics, Department of Biomedical Engineering, Huazhong University of Science and Technology, Wuhan 430074, China

[3]Department of Neurosurgery, USA

[4]Department of Neurology and Neurological Sciences, USA

[5]Stanford University School of Medicine, USA

[#] These authors contributed equally to this work.

SUMMARY

Dynamic adaptations in synaptic plasticity are critical for learning new motor skills and maintaining memory throughout life, which rapidly decline with Parkinson's disease (PD). Plasticity in the motor cortex is important for acquisition and maintenance of novel motor skills, but how the loss of dopamine in PD leads to disrupted structural and functional plasticity in the motor cortex is not well understood. Here, we utilized mouse models of PD and 2-photon imaging to show that dopamine depletion resulted in structural changes in the motor cortex. We further discovered that dopamine D1 and D2 receptor signaling were linked to selectively and distinctly regulating these aberrant changes in structural and functional plasticity. Our findings suggest that both D1 and D2 receptor signaling regulate motor cortex plasticity, and loss of dopamine results in atypical synaptic adaptations that may contribute to the impairment of motor performance and motor memory observed in PD.

Correspondence should be addressed to Dr. Tonghui Xu (xutonghui@hust.edu.cn) Britton Chance Center for Biomedical Photonics, Wuhan National Laboratory for Optoelectronics-Huazhong University of Science and Technology, MoE Key Laboratory for Biomedical Photonics, Department of Biomedical Engineering, Huazhong University of Science and Technology, Wuhan 430, China Dr. Jun B. Ding (dingjun@stanford.edu) Department of Neurosurgery, Department of Neurology and Neurological Sciences, Stanford University School of Medicine, 1050 Arastradero Rd, Building A, Palo Alto, CA, 94304; 1-650-723-5222 (Tel) 1-650-725-7813 (Fax)..

Authors Contributions: T.X. and J.B.D. designed the experiments, performed pilot experiments, and supervised the project. L.G., H.X.,Y.C., Y.S., and T.X. performed *in vivo* imaging experiments, J.I.K and J.B.D. performed the electrophysiology experiments, Y.W.W. performed 2-photon uncaging experiments. T.X., R.R.L. and J.B.D. wrote the manuscripts with contributions from all authors.

Keywords

glutamatergic synapse; dendritic spine; motor cortex; synaptic plasticity; dopamine; Parkinson's disease

INTRODUCTION

The loss of midbrain dopaminergic neurons is the hallmark of Parkinson's disease (PD), a condition characterized by deficits in both fine movement control and motor learning. While the decline in movement control in PD has been linked to alterations in basal ganglia plasticity [1], the deficiencies in motor learning remain largely unexplored. The basal ganglia receive major glutamatergic inputs from the primary motor cortex (M1), a region that is essential for motor control and the acquisition of novel motor skills [2]. M1 cortical neurons have both D1 and D2 classes of dopamine receptors [3,4] and receive direct dopaminergic projections from the ventral tegmental area (VTA) and substantia nigra pars compacta (SNc) via mesocortical pathways [5]. Dopaminergic terminals from the mesocortical pathway richly innervate M1 dendritic processes in both superficial and deep layers of the rodent and primate cortex [6,7], and activation of this pathway could directly modulate M1 cortical activity. It has been shown that stimulation of dopaminergic projections induces activity-dependent *c-fos* expression in M1 [2], and, using voltage-sensitive dye imaging, this evoked neuronal activity has been shown to extend throughout the M1 region [8]. In addition, dopaminergic signaling within M1 modulates the synaptic plasticity of horizontal, intra-cortical connections and is important for optimizing motor skill learning [9]. Because proper M1 processing is essential for motor learning, altered M1 plasticity may be the key mechanism underlying the severe motor learning deficits observed in PD [10]. However, very little is known about dopamine depletion-induced synaptic adaptations in the motor cortex *in vivo*, particularly in relation to structural and functional plasticity in M1 during the progression of PD.

The formation and maintenance of memories involve long-term synaptic structural and functional plasticity. Structural synaptic plasticity generally occurs at dendritic spines [11], and recent studies suggest that functional synaptic plasticity, such as long-term potentiation (LTP) and long-term depression (LTD) can be accompanied by these structural changes at dendritic spines. For example, studies have shown that LTP-like stimulation can induce *de novo* spine formation [12,13] and enlargement of spine volume [14]. Conversely, LTD induction protocols can induce spine shrinkage and spine elimination [15,16]. In the motor cortex, synaptic structural changes have been shown to be associated with enhancement (LTP) or reduction (LTD) of synaptic efficacy [17,18]. The learning of new motor skills can lead to spine genesis and remodeling, and these *de novo* spines are preferentially stabilized during subsequent training, ensuring long-term memory storage [19,20]. In addition, there is strong evidence that blocking dopamine receptors in M1 can abolish LTP induction in M1 superficial layers and can impair motor learning [2,9]. Despite substantial support for direct, pathological changes in the M1 motor cortex in PD [10,21], little is known about how dopamine regulates motor cortex physiology, specifically, how dendritic spine dynamics and

synaptic functional plasticity are altered by the loss of dopaminergic innervation and what the relationship is between them.

To address these fundamental questions, we investigated the process of dopamine depletion-induced synaptic remodeling in the intact motor cortex by repeatedly imaging the apical dendrites of layer V pyramidal neurons. Neurons were identified by expression of yellow fluorescent protein (Thy1-YFP-H line) using trans-cranial two-photon laser scanning microscopy, and dendritic spines were studied over time. We found dramatic increases in both spine elimination and formation in PD mouse models. In addition, we elucidated distinct roles for D1 and D2 dopamine receptors in the M1 motor cortex: D1 receptor signaling regulated spine elimination, while D2 dopamine receptor signaling was linked to spine formation. We also provided evidence for the dissociation between functional LTP/LTD and spine elimination and *de novo* spine formation in the motor cortex, pointing instead towards a novel mechanism by which neuronal activity and dopamine modulate functional and structural plasticity at excitatory synapses. Lastly, we demonstrated that dopamine depletion impairs performance during new motor skill learningand learning-induced spine dynamics. Together, our studies reveal unique roles for D1 and D2 dopamine receptor signaling in regulating spine dynamics and functional plasticity in M1. Given that these roles are disrupted by dopamine depletion, our study suggests that abnormal spine turnover in the motor cortex may contribute to motor deficits observed in PD.

RESULTS

Dopamine depletion enhances dendritic spine dynamics in the motor cortex

Most excitatory synapses are located at dendritic spines, and changes in spine morphology and dynamics reflect synaptic plasticity[11]. Structural remodeling is enhanced during experience-dependent learning and memory [22,23], as well as during pathological changes associated with neurodegenerative and neurological diseases [24,25]. These structural changes in both normal and disease states highlight massive adaptations that result in the constant rewiring of neural circuits. To investigate the process of dopamine depletion-induced synaptic remodeling, we used trans-cranial, two-photon laser scanning microscopy to repeatedly image the same apical dendrites of layer V pyramidal neurons labeled by expression of yellow fluorescent protein (Thy1-YFP-H line) in the forelimb area of the motor cortex. By comparing the images taken from two time points in the superficial layers of the motor cortex, spines were identified as newly formed (arrowheads), eliminated (arrows), filopodia (asterisk) or stable (Fig. 1**a–c**).

We used the 1-methyl-4-phenyl-1,2,3,6-tetrahydropyridine (MPTP)-treated mouse model of PD to investigate whether structural plasticity is altered in adult motor cortex after chronic lesion of dopamine neurons. MPTP-treated mice are commonly used as an animal model to study the pathogenesis and therapy for PD [26] and are generated by administering MPTP (i.p., 30 mg/kg, once daily), a neurotoxin that is taken up by dopamine neurons which leads to selective loss of dopaminergic neurons. Consistent with previous observations, MPTP treatments induced significant and progressive loss of TH-positive dopaminergic neurons in the midbrain area, but not TH-positive noradrenergic neurons in the locus coeruleus (Supplementary Fig. 1 and Supplementary Fig. 2). We imaged the same dendrite segments

before and after 4 days of successive MPTP treatment and found that both spine elimination and formation in the motor cortex of adult (> 2 months old) mice were significantly increased with treatment Fig. 1**c,d,f–g** and Supplementary Table 1). These results were confirmed using reserpine-treated mice, another commonly used PD animal model. Reserpine-injection for 4 days (i.p., 3 mg/kg, once daily) induced similar increases in both spine formation and spine elimination in adult mice (Fig. 1e–g and Supplementary Table 1).

Because spines in the motor cortex of young mice normally exhibit higher plasticity than adults, we next investigated if neural circuit remodeling in the adolescent motor cortex is also influenced by dopamine depletion. We examined spine turnover in adolescent (one month old) mice and found that both spine elimination and formation were also enhanced dramatically after 4 days of MPTP treatment (Fig. 1**h,i** and Supplementary Table 1). To examine if dopamine depletion causes global enhancement of spine dynamics in other cortices, we performed the same experiments in the neighboring barrel cortex of adult mice, but found no significant change in either spine elimination or formation after 4 days of MPTP treatment (Fig. 1**j,k** and Supplementary Table 1). Together, these data suggest that dopamine depletion causes dramatic enhancement of spine remodeling in the M1 motor cortex.

Dopamine depletion induced reorganization leads to unstable neuronal circuits in the motor cortex

To further understand how acute and prolonged dopamine depletion affects spine dynamics, we extended the period of MPTP administration and imaged mice over different periods of time (Fig. 2**a–c**). We found that a single MPTP injection was enough to cause a significant increase in spine elimination and formation in the motor cortex within one day (Fig. 2**d,e** and Supplementary Table 1). Administration of MPTP for longer periods of 8, 12 and 16 days resulted in consistent and cumulative increases in spine dynamics (Fig. 2**b–e** and Supplementary Table 1). Based on the changes in elimination and formation rate, we calculated total spine numbers to assess if total spine density is altered following dopamine depletion. Because both elimination and formation were enhanced by dopamine depletion, only a modest decrease in total spine number was observed in the M1 motor cortex following chronic MPTP treatment when compared to control mice (Fig. 2**f**). This is despite the fact that the total spine turnover (sum of spine elimination and formation) was dramatically increased (Fig. 2**g**).

Enhanced spine formation and elimination reflect rewiring of neuronal circuitry in response to loss of dopamine. To further examine the time course of this reorganization, we imaged each dendrite at three time points. New, lost, and pre-existing spines were defined by their appearance or disappearance between the first and second images, taken at day0 or day 4. Spines were then monitored for their final fate in the third image, taken at day 8, 12, or 16. In PD mouse models, pre-existing spines became significantly less stable than those in control mice over the same time periods: fewer pre-existing spines remained in MPTP-treated mice. During the same period of time in control mice, the majority of the pre-existing spines remained stable (Fig. 2**h**). Together, these data indicated that dopamine depletion

triggers rapid and persistent remodeling of neural circuitry in the motor cortex. The net effect is that the pre-existing synaptic connections became unstable.

D1 and D2 dopamine receptor signaling differentially regulate spine elimination and formation

Exogenously administered L-3,4-Dihydroxyphenylalanine (L-DOPA), the endogenous precursor of dopamine, is presently the most widely used drug for treating PD patients. To confirm the involvement of dopamine in structural plasticity in the motor cortex we examined if L-DOPA could reverse the enhanced spine dynamics seen in MPTP-treated mice. We treated mice with MPTP once daily for four consecutive days, followed by another four day treatment of L-DOPA (i.p., 100 mg/kg, once daily) combined with MPTP (Fig. 3**a**). We found that L-DOPA can partially rescue the enhancement of spine elimination and formation caused by MPTP. Although the rate in spine turnover was still larger in MPTP and L-DOPA-treated animals compared to saline injected controls, the increases in the elimination and formation rates induced by MPTP with L-DOPA administration were significantly lower than those by MPTP injection alone (Fig. 3**b**). These results confirm that the enhancement in motor cortex spine dynamics observed in MPTP mice is dependent on dopamine depletion.

Dopamine exerts its function through intracellular G-protein coupled receptor-signaling cascades. There are two major classes of dopamine receptors[27]: the D1 class, which is coupled to Gs signaling and the D2 class, which is coupled to Gi/o signaling. Activation of D1 receptors leads to increases in cytosolic cAMP levels and activation of protein kinase A (PKA), while activation of D2 receptors leads to inhibition of cAMP. To further understand how distinct dopamine receptor signaling is involved in regulating spine dynamics in the motor cortex, we examined spine elimination and formation in adult mice treated with the D1 receptor antagonist SCH23390 or the D2 receptor antagonists Haloperidol and Raclopride (Fig. 3**a**). Surprisingly, we found that D1 receptors are uniquely involved in spine elimination and D2 receptors are uniquely involved in spine formation. SCH23390 (0.25mg/kg i.p., twice daily) significantly promoted spine elimination but had no effect on spine formation in the same animals (Fig. 3**c,d,f**, and Supplementary Table 1). In stark contrast, Haloperidol (3 mg/kg i.p., once daily) and Raclopride (0.4 mg/kg, i.p., twice daily) did not change spine elimination rates, but significantly increased the rate of spine formation (Fig. 3**e,f**, Supplementary Fig.2, and Supplementary Table 1). It is worth mentioning that the increase in spine elimination by D1 antagonist mimicked the changes in spine elimination observed in MPTP-treated mice (P=0.9197, compared to MPTP, Mann-Whitney), while the increase in spine formation by D2 antagonist resembled the alterations in spine formation rate in MPTP-treated mice (P=0.8016, compared to MPTP, Mann-Whitney). Because D1 antagonists promoted spine elimination without affecting formation, SCH23390 treatment resulted in an obvious reduction in spine density compared to MPTP. In contrast, Haloperidol treatment resulted in a significant increase in spine density (Fig. 3**g**). In addition, prolonged treatment with D1 or D2 antagonists also promoted consistent and cumulative increases in spine elimination or formation, respectively (Fig. 3**h**, and Supplementary Table 1). As expected, the consistent increases in spine elimination and formation with these treatments resulted in further alterations in spine density (Fig. 3**i**

Together, these results suggest that L-DOPA can partially rescue the enhanced spine turnover seen in PD mouse models, and distinct dopamine receptor activity is critical in maintaining proper spine dynamics.

Spine turnover is regulated by direct dopaminergic projections in M1

Pyramidal neurons in M1 express both D1 and D2 classes of dopamine receptors [3,4]. Dopaminergic modulation of M1 can arise from two anatomically and functionally distinct pathways: mesocortical or nigrostriatal projections. Mesocortical afferents project directly to the M1, play an important role in motor learning and have the potential to critically modulate synaptic and structural plasticity in M1 [2,9]. On the other hand, nigrostriatal afferents indirectly project to the M1 via the basal ganglia, and are critically involved in movement execution [28]. The nigrostriatal system exerts powerful modulation on the direct and indirect pathways of the basal ganglia, in which direct pathway striatal projection neurons (SPNs) express D1 receptor and indirect pathway SPNs express D2 dopamine receptor [29]. The substantia nigra reticulata (SNr), the output of two striatal pathways, provides inhibition to the thalamus, which subsequently excites the cortex through glutamatergic synapses. Thus, nigrostriatal projections can indirectly modulate structural plasticity in the motor cortex through cortex-basal ganglia-thalamus closed-loop feedback.

To directly test these two possibilities, we combined *in vivo* imaging experiments through open-skull chronic cranial windows with subsequent focal dopaminergic terminal lesions. We turned to open-skull cranial windows, because intracranial injections compromise the bone structure, which prevents us from using the thinned-skull preparation for *in vivo* imaging. After imaging dendritic structures through a chronic cranial window, we selectively eliminated dopaminergic terminals either in the forelimb area of the M1 or the dorsal lateral striatum by stereotaxic local injection of the neurotoxin 6-hydroxydopamine (6-OHDA) (Fig. 4**a,b**). The denervation of dopaminergic terminals in M1 and striatum was verified by immunostaining for tyrosine hydroxylase (TH). TH immunofluorescence in M1 cortical layers was nearly absent in the ipsilateral hemisphere 8 days after M1 6-OHDA injections, while TH signals in the striatum were comparable to those of the contralateral side (Fig. 4**c** and Supplementary Fig. 4). In contrast, TH signal in M1 was only slightly reduced (~30% reduction in TH immunofluorescence intensity, n=5) as compared to the non-injected contralateral hemisphere following striatal 6-OHDA injection (Fig. 4**d** Supplementary Fig. 3).

We imaged the same dendrite segments through the cranial window before and 8 days after 6-OHDA intracranial injection, and found that both spine elimination and formation in the motor cortex were significantly increased following M1 6-OHDA lesion. In order to assess the effect of eliminating dopaminergic terminals in the dorsal lateral striatum, we injected 6-OHDA into both the M1 and the striatum. The results showed no further enhancement in either spine elimination or formation compared to M1 6-OHDA lesion models (Fig. 4**e** and Supplementary Table 1). Together, these data suggest that loss of dopamine promotes spine elimination and formation in M1 primarily through local mechanisms primarily involving direct mesocortical projections, although we cannot exclude the possibility that basal ganglia pathways may also contribute to the effect.

Dopamine regulation of long-term potentiation (LTP) and long-term depression (LTD)

Our data from the 6-OHDA local lesion experiments suggested that primarily local synaptic mechanisms are involved in spine remodeling in M1. Therefore, we next tested if synaptic plasticity at glutamatergic synapses in layer V pyramidal neurons is compromised following dopamine depletion. Many lines of evidence suggest that structural plasticity is a reflection of, or is caused by, functional, long-term changes in synaptic efficacy. A simple, parsimonious model is that long-term potentiation (LTP) stimulates spine formation, while long-term depression (LTD) promotes spine elimination [12–16]. In addition, LTP is important for stabilizing newly formed spines along with inducing spin their growth [30]. Our data demonstrate that dopamine depletion enhances both spine elimination and formation by reduced D1 and D2 receptor activity, respectively. This, suggest that dopamine may control synaptic long-term plasticity through these two different classes of receptors in the motor cortex. To directly test this hypothesis, and to determine whether D1 and D2 signaling is involved in LTP and LTD induction, we performed whole-cell patch clamp recordings from identified neurons in the M1 motor cortex from young adult Thy1-YFP-H mice. We placed stimulation electrodes in the superficial layer of the cortex and used minimal stimulation to activate superficial layer inputs on layer V pyramidal neurons (Fig. 5**a**). Consistent with previous findings [31], presynaptic stimulation paired with postsynaptic depolarization (pairing protocol) reliably induced LTP in layer V pyramidal neurons in the motor cortex, and was completely blocked by NMDA-receptor blocker R-CPP (10 μM) (Fig. 5**b**–**f**. To our surprise, LTP induction was impaired in dopamine-depleted mice by both reserpine injections and 6-OHDA lesions (Fig. 5**g**–**i**). To test if the changes in spine dynamics were M1 specific, we assessed if LTP induction in the neighboring barrel cortex would also be affected by dopamine depletion. Consistent with our data on structural plasticity in the barrel cortex, we found that LTP induction in the barrel cortex was not impaired in reserpine-injected mice (Supplementary Fig. 5).

To further understand how dopamine receptor signaling is involved in LTP in the motor cortex, we perfused brain slices with D1 and D2 receptor blockers. We found that LTP was specifically blocked by the D1 receptor antagonist (SCH23390, 3 μM) (Fig. 5**j,l**), but was not affected by the D2 receptor antagonist (Sulpiride, 5 μM) (Fig. 5**k,l**). On the other hand, LTD could not be elicited by paring low-frequency stimulation (LFS) with slight membrane depolarization (Fig. 6**a**), which was consistent with previous findings that showed that LTD induction is age-dependent [32]. LTD induction was also absent in dopamine depleted mice (Fig. 6**b**–**d**). Notably, the same pairing LTD protocol successfully induced LTD in brain slices from young adolescent mice (3 weeks old). This form of LTD in young adolescent animals was impaired after reserpine injection (Fig. 6**e,f**). Together, our results indicate that D1, and not D2, receptor activation is required for LTP, and dopamine depletion impairs LTP induction at the superficial layer synapses on layer V pyramidal neurons. LTD in young adolescent mice was also affected by dopamine depletion. However, LTD elicited by the pairing protocol was absent in the motor cortex of adult mice, suggesting LTD may not directly contribute to changes in spine dynamics in adult mice.

Dopamine regulates structural and functional plasticity in the motor cortex

What could dramatically promote spine elimination and formation without enhancing LTP and LTD in parallel? One possibility is that LTP and LTD may be occluded following dopamine depletion, as spines are already at maximum capacity of functional plasticity. If this were true, then aberrant synaptic plasticity could prevent spines from undergoing further formation and elimination. However, the sustained and cumulative change in spine turnover during prolonged dopamine depletion (Fig. 2) argues against this hypothesis. Instead, our data implies that spines represent readily available substrates for structural plasticity that do not necessarily correlate with functional long-term synaptic plasticity. This points to a new model for dopamine regulation of structural and functional plasticity in the adult motor cortex: *de novo* spine formation and elimination are dissociated from functional long-term plasticity, and instead are distinctly regulated by D1 and D2 receptor signaling (Supplementary Fig. 6). D2 receptor signaling is selectively linked to spine formation, while D1 receptor signaling is selectively linked spine stabilization and elimination. Furthermore, this model emphasizes that LTP shares a common mechanism with stabilization of dendritic spines but not necessary for spine formation and, conversely, lack of LTP would promote spine elimination [30]. This model supports our results, which demonstrate that dopamine signaling, specifically through D1 receptor activation, is required for LTP. Functionally, chronic dopamine depletion or blockade of D1 receptors abolished LTP induction, while structurally, it promoted spine elimination. In parallel, chronic dopamine depletion or D2 receptor blockade promoted spine formation without involvement of functional synaptic potentiation. This model predicts that LTD is not required for spine elimination, which is consistent with previous findings which show that LTD induction in many cortical regions is reduced or absent in the adult brain. This model also highlights the important role of LTP in spine remodeling during motor learning. Novel experiences and activities resulting in new spine formation, together with LTP-induced spine stabilization, and experience-dependent pruning, represent a stable structural and functional synaptic mechanism for memory storage. In PD, due to loss of both D1 and D2 receptor activation, both synapse elimination and formation are dramatically enhanced.

This paradigm highlights the idea that structural plasticity following dopamine depletion is mediated by local changes in the M1 cortex. If we can precisely induce spine formation in M1 layer V pyramidal neurons without involving feedback from basal ganglia output, we should be able to enhance spine formation by blocking D2 receptors. By triggering glutamate release via 2-photon laser uncaging, a recent study showed that *de novo* spine growth from the dendritic shaft can be induced with high spatial and temporal precision, and furthermore, these newly formed spines can form functional synapses with nearby axonal boutons [13]. To determine if *de novo* spine formation is regulated by D1 and D2 receptors in M1, we used both 2-photon microscopy to image the apical dendrites of layer V pyramidal neurons, and 2-photon uncaging of MNI (4-methoxy-7-nitroindolinyl)- glutamate to release glutamate at specific dendritic locations (Supplementary Fig. 7). Because dopamine is critically involved in initial synaptogenesis during the second postnatal week (postnatal day 7–14) *in vivo* [33], we performed our analysis in acute cortical brain slices from young Thy1-YFP-H mice (postnatal day 15–18). Stimulation was applied to aspiny stretches of secondary and tertiary dendrites (Fig. 7a). Stimulation by 40 pulses (0.5 ms) of uncaging

laser at 5 Hz induced growth of a new spine with a success rate of ~12 % (n = 121) (Fig. 7b–c, Supplementary Movie 1 and 2). We found that blocking D1 receptor activation by bath-application of SCH23390 (3 μM) did not affect the success rate of spinogenesis (Fig. 7c), which is consistent with our *in vivo* imaging results. Conversely, inhibiting D2 receptor activation by Sulpiride (5 μM) and Haloperidol (2 μM) significantly enhanced the success rate of spinogenesis (Fig. 7c), indicating that D2 receptor signaling serves as a checkpoint for preventing excessive spinogenesis. Consistent with previous findings, we found that preventing NMDA receptor activation by R-CPP (10 μM) nearly abolished spinogenesis (Fig. 7c). It is worth mentioning that blocking LTP by a use-dependent NMDA receptor blocker, MK801, did not abolish the spinogenesis, though there was a trend suggesting a decreased success rate (Fig. 7c). This suggests that the initial Ca^{2+} entry through NMDA receptors in the presence of MK801 is sufficient to induce spinogenesis. Together, these data indicate that indeed, D2 receptor signaling in the motor cortex is directly associated with spinogenesis without requiring LTP: blocking D2, but not D1, receptor activation dramatically enhanced the rate of successful spinogenesis.

Our proposed model also suggests that the lack of LTP could promote spine elimination, and potentially decreased survival rates of newly formed spines. To investigate this, we tracked newly formed spines following MPTP and dopamine receptor antagonist injections and analyzed their survival rates (Supplementary Fig. 8). Indeed, the survival rate of newly formed spines in MPTP-injected mice were significantly lower than that of Haloperidol-injected mice, which could be attributable to loss of LTP in MPTP-injected mice. In order to directly test whether blocking LTP could lead to changes in spine dynamics in the motor cortex, we examined spine elimination and formation in mice treated with MK801 (0.5 mg/kg, twice daily), an NMDA receptor blocker that crosses the blood-brain barrier and potently blocks LTP induction. We found that MK801 indeed significantly promoted spine elimination, but had no significant effect on spine formation in the same animals (Fig. 7d and Supplementary Table 1). Together, our data demonstrate the unique role of long-term synaptic plasticity in spine dynamics *in vivo*.

These aberrant synaptic adaptations resulting from the degeneration of mesocortical projections to the M1 may explain why PD patients have impaired skill learning and memory retention [34]. We directly tested this hypothesis by investigating the relationship between performance of motor skill tasks and structural plasticity in the motor cortex following dopamine depletion. To do so, we trained mice to perform a food pellet reaching task[19]. During training, control 2-month-old mice gradually increased their reaching success rates in the initial 4 days, after which their success rates plateaued. In comparison, mice pre-treated with 4 days MPTP injections exhibited significantly decreased success rates (from day 5 to day 8, Fig. 8a–c). We housed the same cohort of mice in their home cage for one month after their eight-day training period, and then tested their performance in the food pellet reaching task. We found that pre-trained control mice maintained skillful performance with high success rates on day 38. However, pre-trained MPTP-injected mice showed decreased success rates (Fig. 8c). Together, these data suggest that, indeed, motor skill is impaired following dopamine depletion.

To investigate the process of learning-induced remodeling of neural circuits in the M1 motor cortex and the adaptation of synaptic mechanisms in PD mouse models, we repeatedly imaged the same dendritic regions of layer V pyramidal neurons through a cranial skull window. Motor learning induced a transient increase in the formation of dendritic spines accompanied with enhanced spine elimination in the motor cortex contralateral to the reaching forelimb in control mice (Fig. 8d–e, and Supplementary Table 2). These data are consistent with previous reports demonstrating that motor skill learning can induce rapid formation of dendritic spines followed by selective pruning [19,20]. Interestingly, MPTP-injected mice that underwent the same motor skill training did not show significant increases in spine formation when compared to naïve MPTP-injected mice; in addition, enhancement of spine elimination after training was also impaired.

Previous studies have shown that learning-induced newly formed spines are preferentially stabilized during training and endure even after training stopped, thus providing neural substrate for long-lasting motor memory [19,20]. LTP plays a critical role in stabilizing dendritic spines, and it is possible that, in MPTP-injected mice, LTP is impaired following loss of dopamine, leading to failures in stabilizing the newly formed, learning-induced spines. To directly test whether spine stabilization is indeed impaired, we analyzed the fate of newly formed spines during and after motor training in control and MPTP-injected mice. We found that, in control mice, learning-induced, newly formed spines were significantly more stable (Fig. 8h), which is consistent with previous findings. At the initial training phase, new spines were more stable in trained MPTP-injected mice than in MPTP-injected naïve mice. However, most of the new spines in the MPTP-injected, trained mice were then eliminated, and the spine survival rate became not significantly different from MPTP-injected naïve mice. Taken together, these data indicate that dendritic spines on layer V pyramidal neurons in the motor cortex undergo rapid structural remodeling following dopamine depletion. In addition, selective stabilization of learning-induced, newly formed spines was clearly impaired, as most of these spines were unable to be converted into stable synapses following dopamine depletion. Learning-induced rewiring was unable to undergo stabilization, presumably because of impairments in functional plasticity, such as LTP. The impairment in stabilization of neural circuits provides an additional synaptic mechanism for the motor deficits seen in PD.

DISCUSSION

PD results from the degeneration of midbrain dopaminergic neurons, and the majority of research to date has focused on synaptic adaptations in the striatum, a region that receives the highest density of dopaminergic innervation [35]. Cortical areas, on the other hand, have received very little attention, even though the motor cortex, which is the command center that governs precise fine motor control, also receives rich projections from midbrain dopamine neurons [36]. In this study, we investigated dendritic spine mobility and functional plasticity in the motor cortex in PD. We showed that both spine elimination and formation in M1 are significantly increased in PD mouse models. Activity of M1 can be either directly elicited by activating mesocortical dopaminergic projections [2], or indirectly modulated by nigrostriatal projections through the basal ganglia-thalamus-cortex close-loop feedback system [37]. Our data indicate that structural and functional plasticity in M1 is mainly

influenced by the activity of mesocortical dopaminergic direct projections. The rewiring in the motor cortex was uniquely regulated by D1 and D2 dopamine receptors in the M1 motor cortex: D1 receptor signaling was directly linked to spine elimination, while D2 dopamine receptor signaling was directly linked to spine formation. Therefore, spine formation and elimination, two distinct structural plasticity mechanisms, are dissociable at the dopamine receptor level. In addition, we revealed a novel relationship between LTP/LTD, spine elimination and *de novo* spine formation. Furthermore, by combining motor skill training and *in vivo* imaging, we demonstrated that dopamine depletion impaired performance of newly learned motor skills, and compromised learning-induced spine dynamics and selective stabilization in the motor cortex. The motor cortex plays critical roles in movement control, and given that these roles are regulated by the mesocortical dopaminergic system and disrupted by dopamine depletion, our study suggests that abnormal spine turnover in the motor cortex may contribute to motor deficits observed in PD.

Role of D1 and D2 signaling in regulating functional and structural plasticity

Dopamine exerts its function through activating G-protein coupled receptors. Two major classes of dopamine receptors are expressed in M1: the D1 class, which is coupled to Gs signaling and the D2 class, which is coupled to Gi/o signaling [3,4]. In the present study, we showed that D1 and D2 receptors have their distinct roles in regulating dendritic spine elimination and formation. In particular, D1 receptor signaling was selectively linked to spine elimination, while D2 dopamine receptor signaling was selectively linked to spine formation. Interestingly, blocking D2 receptor activity and depleting dopamine in mouse models of PD promoted spine formation. How activation of D1 and D2 receptors lead to downstream intracellular signaling cascades that regulate spine dynamics is not well understood. Activation of D1 receptors leads to an increase in cytosolic cAMP level and activation of protein kinase A (PKA), and conversely, activation of D2 receptors leads to inhibition of cAMP and decrease of PKA activity. A recent study showed that activity induced spinogenesis can be bi-directionally regulated by PKA [13]. It is therefore possible that PKA activity is involved in regulating spine dynamics in M1 following dopamine depletion. Dopamine neurons fire action potentials spontaneously, which provide tonic dopamine release in targeted areas. Moreover, dopamine neurons can switch from low-frequency tonic activity to phasic bursts of action potentials. Such firing patterns could encode reward prediction errors and incentive salience [38], which are critical for motor skill learning. D2 receptors have higher binding affinity to dopamine and can be preferentially activated during tonic dopaminergic neuron activity. Therefore, tonic activation of D2 receptor may serve as a checkpoint for preventing ectopic growth of dendritic spines that are irrelevant to experience. During reward-based associative learning, phasic dopamine neuron firing will enhance dopamine release and activate low-affinity D1 receptors. Activation of D1 receptors may enhance synaptic connections by regulating the function and trafficking of AMPA and NMDA receptors [39]. Consistent with this notion, we found that the D1 receptor is critically involved in LTP induction, which may be required for stabilizing dendritic spines and encoding motor memory during skill learning [9]. Loss of D1 receptor activation may compromise the consolidation of motor memory and may destabilize pre-existing synapses. Therefore, changes in spine dynamics in mouse models of PD can be explained by the simultaneous loss of D1 and D2 receptor activation following dopamine depletion: an

increase in spine elimination by D1 antagonism mimicked the changes observed in spine elimination in MPTP-treated mice, and an increase in spine formation by D2 antagonism resembled the increase in spine formation rates in MPTP-treated mice. It is worth noting that D1 receptor activation also contributes to LTP at corticostriatal synapses. Abnormal information storage in these synapses is linked to the development of L-DOPA-induced dyskinesia [40].

Relationship between functional and structural plasticity

One existing model for synaptic plasticity is that long-term potentiation (LTP) stimulates spine formation while long-term depression (LTD) promotes spine elimination, and many lines of evidence support this theory [12–16,41]. However, these previous studies may have overlooked the issue of age, as synapses can undergo bi-directional plasticity through early development stages. In addition, LTP promotes the transition of nascent spines to persistent stable spines [30].

Interestingly, we found that spine formation was enhanced in our PD paradigms, even though LTP was blocked by dopamine depletion. We also found that LTD had a minimal presence in the adult cortex, even though dendritic spines continued pruning. Together this, suggests the dissociation between LTD and spine elimination. Therefore, our findings provide an alternative interpretation for dopamine regulation of structural and functional plasticity in the adult motor cortex.

This explains our results, which demonstrate that dopamine signaling, through D1 receptor activation is required for LTP. Functionally, chronic dopamine depletion or blockade of the D1 receptor prevented LTP induction, while structurally, it promoted spine elimination. In parallel, chronic dopamine depletion or D2 receptor blockage promoted spine formation, without involving functional synaptic potentiation. In PD, due to the concurrent loss of both D1 and D2 receptor activation, both synapse elimination and formation in M1 are dramatically enhanced, decreasing synaptic stability. In addition, performing a newly learned motor skill failed to induce further enhancement of spine turnover in MPTP-injected mice.

Involvement of Motor Cortex in PD

Patients with PD have deficits in skill learning [34], and although this disease is mostly characterized by degradation of the nigrostriatal dopaminergic system, extrastriatal dopaminergic neurons and other monoamine systems also degenerate, particularly as the disease progresses. PD patients show reduced ^{18}F-dopa uptake in the motor cortex, which has been used as a marker for the degradation of cortical dopaminergic terminals [42]. Degeneration of mesocortical projections to M1 may contribute to the synaptic adaptations and skill learning deficits in PD human patients.

The primary motor cortex not only provides major glutamatergic afferents to the input nucleus of the basal ganglia, but it is also a major target of the basal ganglia output; therefore, this region likely transforms patterns of pathological activity into the motor symptoms in PD. There have been few studies investigating the synaptic adaptations and neuronal activities in the primary motor cortical neurons in PD [9,43–45]. Our findings show

that there were dramatic changes in synaptic dynamics in M1 following dopamine depletion. The consequence of structural remodeling is a net loss of stable spines in layer V pyramidal neurons in PD. Interestingly, our study further showed that a new skill training paradigm failed to enhance spine formation and elimination, and failed to stabilize learning-induced new spines in MPTP-treated mice. Together, the abnormally enhanced dynamics of neural circuitry and the destabilization of both pre-existing and learning-induced newly formed spines in response to dopamine depletion may together contribute to motor deficits in PD.

Recent studies suggest that neuronal activities in M1 layer V pyramidal neurons undergo drastic changes at both the single-cell and the population level in Parkinsonian mice Therapeutic deep brain stimulation (DBS) targeting the subthalamic nucleus (STN) could directly interfere with pathological cortical oscillations in PD [45]. In addition, a recent study showed that manipulation of STN neuronal activity by optogenetic stimulation was not sufficient to produce therapeutic effects in mice with PD. In contrast, stimulation of the layer V neurons in M1 or in their axons was beneficial for restoring motor ability [46]. Together, an important role of the motor cortex is emerging in a picture that has important implications for both pathology and treatment strategies for PD: the direct modification of abnormal synaptic plasticity and neuronal activities in the motor cortex could have a major therapeutic effects for PD patients.

MATERIALS AND METHODS

Animals

All procedures were approved by Stanford University's Administrative Panel on Laboratory Animal Care. Adult (1–3 months) mice (male or female) were used for *in vivo* imaging and electrophysiology, and postnatal day 15-18 (p15-18) mice (male or female) were used for *de novo* spinogenesis experiments. Transgenic mice expressing YFP in a small subset of cortical neurons (Thy1-YFP-H line, Jackson Laboratory, JAX #003782) [47] were purchased from Jackson Laboratory, housed, and bred in the animal facilities at Stanford University and Wuhan National Laboratory for Optoelectronics with normal 12 hr light/dark cycle. Animals were randomly assigned to either control saline or drug treatments. All animal experiments were carried out in compliance with protocols approved by Stanford University's Administrative Panel on Laboratory Animal Care, the Hubei Provincial Animal Care and Use Committee and the experimental guidelines of the Animal Experimentation Ethics Committee of Huazhong University of Science and Technology, China.

Thin skull surgical procedure

The procedure of transcranial two-photon imaging was modified from Yang et. al [48]. Mice were anesthetized via intraperitoneal injection with a cocktail of 17 mg/ml Ketamine and 1.7 mg/ml Xylazine, or a cocktail of 2% Chloral hydrate, 8% Urethane and 1.7 mg/ml Xylazine in 0.9% NaCl. After resecting the scalp to expose the skull and remove the periosteum, the skull above the cortical region of interest was manually thinned using either a high-speed micro-drill or a microsurgical knife under a dissection microscope. The skull was kept cool by periodically dropping sterile saline solution on the surface to avoid friction-induced

overheating, which may damage the underlying cortex. The thinned region for imaging was ~200 μm in diameter and ~20 μm in thickness.

Surgical procedure for implanting chronic cranial windows

Mice aged 45 days were anesthetized with an intraperitoneal injection containing 2% Chloral hydrate, 8% Urethane and 1.7 mg/ml Xylazine in 0.9% NaCl. The head of the animal was stabilized in a stereotaxic frame. The skin and periosteum were removed to expose the skull from olfactory bulb to cerebellum. A high-speed drill was used to drill a circular groove in the skull above primary motor cortex. Drilling was intermittent for heat dissipation and a cool sterile solution was periodically added to the skull to avoid friction-induced heat damaging the underlying cortex. When the island of cranial bone moved responding to being touched lightly by a drill head, it was removed and replaced with a circular cover-glass window. Animals with compromised dura were excluded. A thin layer of superglue was applied to the surface of skull and the edge of cover glass to seal off the exterior, and this was followed by dental resin to cover both exposed skull and wound edge. Finally, a titanium bar with threaded holes was attached on the posterolateral skull of the cranial window for stabilizing the animal head during subsequent imaging sessions. Animals recovered from surgery for at least two weeks before imaging *in vivo*.

In vivo repeated imaging of dendritic spines

For achieving stable, high-resolution imaging, the skull was glued to a stainless steel plate with an opening over the thinned skull, and the plate was fixed to a metal base. Repeated imaging of apical dendritic stretches of L5 pyramidal neurons 10–100 μm below the cortical surface were performed through the thinned area using a custom built, two-photon microscope or an Olympus microscope (FV1200) with a Mai Tai Ti:sapphire laser (Spectra-Physics) at 925 nm with a low laser power (the output optical power <40 mW) to avoid phototoxicity. Stacks of image planes were obtained with a step size of 0.70 μm using a water-immersion objective (Olympus objective). In order to relocate and align the same imaged area at later imaging sessions, the dendritic structures of interest in the low-resolution image stack were taken with a step size of 2.0 μm and the patterns of brain vasculature in the same area imaged with a CCD camera were used as landmarks. The plate was detached from the skull and the scalp was sutured after imaging. Then the animal was returned to its original house cage until the next imaging session. The imaged regions were located according to the stereotactic coordinates and the description from Gan's lab[20]. The location of motor cortex for imaging was 1.2mm lateral from the midline and 1.3mm anterior to the bregma. That of barrel cortex was 3.4mm lateral from the midline and 1.1mm posterior to the bregma.

Identifications of spines and filopodia

Individual dendritic protrusions (length >1/3 dendritic shaft diameter) were tracked manually along dendrites. Conservative criteria were used to define filopodia as long thin protrusions with length/neck diameter >3 and head diameter/neck diameter < 2. Other protrusions were classified as spines. Spine changes, such as the elimination and formation, were determined by comparing images collected at two time points. A stable spine was

considered as such if it was present in both images. Spines were considered the same based on their spatial relationship to adjacent landmarks and/or their position relative to adjacent spines. An eliminated spine was the one that appeared in the initial image, but not the second image. A newly formed spine was the one that was absent in the initial image and then appeared in the second image.

Data quantification and image presentation

All image analysis of spine dynamics was measured manually on the raw image stacks using ImageJ software (NIH ImageJ), blind to the experimental conditions. The same dendritic segments from three-dimensional image stacks with high image quality were used for analysis to ensure that tissue rotation or movements between imaging sessions did not impact identification of the protrusions. Spine heads that contained saturated pixels were excluded. The total number of spines was pooled from the dendritic segments of different mice. The elimination and formation rates of spine were, respectively, the percentages of spines that disappeared and appeared between two imaging sessions, relative to the total spine number of the previous image. Percentages of stable, eliminated, and newly formed spines were all normalized to the initial image. Percentage change in total spine number between sessions was relative to the total number of spines in the first image, and was calculated as plus formation rate, minus elimination rate. Data on spine dynamics throughout our study are presented as mean±SEM. 2D projections of 3D image stacks containing in-focus dendritic segments with high image quality were selected for making all figures. The projected images were thresholded, contrasted, and median filtered for the final figures.

6-OHDA and saline injections

6-OHDA or saline (as control) microinjections were performed after the first imaging session. In brief, 6-OHDA was dissolved with 0.2mg/ml ascorbic acid at a concentration of 4 μg/μl in saline. Anesthetized animals were positioned in a stereotaxic apparatus (STOELTING). A glass electrode filled with 6-OHDA and aimed at M1 or caudate putamen (CPu) was used for injection. The intended stereotaxic coordinates were: AP: −1.0mm; ML: +1.2mm; (with an angle of 30° or 60° from the posterior to the anterior for M1 or CPu, separately); DV: +2.0mm or 0.7 mm for M1 or CPu, separately. Animals were randomly assigned into two groups: one received 100 nl 6-OHDA into the M1 forelimb representation area, the other received 500 nl 6-OHDA injection into the CPu of either hemisphere. The injection was conducted at a rate of 1 μl/30 min, and the glass electrode was left in place for additional 10 min before it was slowly withdrawn over a 10 min time frame. The second imaging session was conducted eight days after injection. Spine dynamics in the motor cortex of 6-OHDA lesioned and saline-injected animals were determined by comparing images from two time points, and then normalizing to the initial images. After the final imaging session, the mice were anesthetized and then transcardially perfused with 4% paraformaldehyde (PFA) in phosphate buffered saline. The cortical and striatal denervation of dopaminergic fibers were determined by tyrosine hydroxylase (TH) staining.

Tyrosine hydroxylase (TH) staining and quantification

Mice were deeply anesthetized and perfused with 4% paraformaldehyde (PFA) transcardially. The brains were removed and post-fixed in 4% PFA for 12h. After cryoprotection in 30% sucrose at 4°C for 2~3 days, brains were sectioned (30μm) encompassing the entire the substantia nigra pars compacta (SNpc) on a cryostat microtome. For cortical and striatal TH-positive fibers study, brain was sectioned (100 μm) on a vibration microtome.

After blocking, sections were incubated in rabbit polyclonal anti-Tyrosine hydroxylase (TH) primary antibody (1:700; Sigma) for 24h at 4°C. After washing three times in PBS, sections were incubated in CY3-conjugated goat Anti-rabbit IgG (1:100, Jackson ImmunoRresearch Laboratories. Inc) secondary antibody for 2h at room temperature, followed by washes in PBS. Numbers of TH-positive neurons were bilaterally counted manually at 5-section intervals throughout the entire extent of SNc/VTA by bright-field microscopy (Nikon Ni-E upright, 10×/0.45,dry,WD 4mm) using ImageJ (NIH) software. To quantify changes in the number of TH-positive neurons in the SNc/VTA regions, the number of TH-positive neurons in control mice was normalized to 100%, and the number of TH-positive neurons in MPTP-treated mice was expressed as a percentage of the control (mean ± SEM). TH-positive fibers in the cortex and striatum were imaged (Nikon A1R MP+ upright, 16×/0.8,water,WD 3mm) and quantified by measuring the optical density of TH immunofluorescence using MATLAB, and the value was reported as the percentage of optical density (mean ± SEM).

Whole-cell patch clamp recording in mouse primary motor cortex (M1)

3~5-week-old Thy1-YFP-H mice (male and female) were anesthetized with isoflurane, decapitated, and briefly exposed to chilled artificial cerebrospinal fluid (ACSF) containing 125 mM NaCl, 2.5 mM KCl, 1.25 mM NaH_2PO_4, 25 mM $NaHCO_3$, 15 mM glucose, 2 mM $CaCl_2$ and 1 mM $MgCl_2$ oxygenated with 95% O_2 and 5% CO_2 (300~305 mOsm, pH 7.4). Coronal slices (300 μm) containing M1 were prepared using a tissue vibratome (VT1200S, Leica), and slices were first maintained in ACSF for 30 min at 34°C and then subsequently recovered at room temperature for 30 min. After recovery, slices were transferred to a submerged recording chamber perfused with ACSF at a rate of 2~3 ml/min, and maintained at 30~31 °C. Picrotoxin (50 μM) was present to block $GABA_A$ receptor–mediated currents. Motor cortex M1 and barrel cortex layer V pyramidal neurons were identified by YFP signal (BX51, Olympus), and EPSCs were induced by stimulating the superficial layer of M1 and barrel cortex via a concentric bipolar stimulating electrode (FHC) in the area. Tissues surrounding the recording area were cut to prevent polysynaptic responses. Whole-cell voltage clamp recordings were made with glass pipettes (3~4 MΩ) filled with an internal solution containing 126 mM CsMeSO3, 10 mM HEPES, 1 mM EGTA, 2 mM QX-314 chloride, 0.1 mM CaCl2, 4 mM MgATP, 0.3 mM Na3GTP, 8 mM Na2-phosphocreatine (280~290 mOsm, pH 7.3 with CsOH), and cells were voltage clamped at −70 mV. EPSCs were evoked at 0.05 Hz and three successive EPSCs were averaged, expressed relative to the normalized baseline. Access resistance was 15~25 MΩ and only cells with a change in access resistance < 20% were included in the analysis. Whole-cell patch clamp recordings were performed using Multiclamp 700B (Molecular Devices), monitored with WinWCP

(Strathclyde Electrophysiology Software) and analyzed offline using Clampfit 10.0 (Molecular Devices). Signals were filtered at 2 kHz and digitized at 10 kHz (NI PCIe-6259, National Instruments). For pairing LTP, conditioning stimulation was delivered within 13 min of achieving whole-cell configuration. After establishing a stable baseline (5 min), presynaptic stimulation (2 Hz, 360 pulses) was paired with postsynaptic depolarization at +10 mV. For pairing LTD, conditioning stimulation was delivered within 30 min of achieving whole-cell configuration. After establishing a stable baseline (10 min), low frequency stimulation (LFS, 1 Hz, 200 pulses) was paired with postsynaptic depolarization at −30 mV. For reserpine experiments, each Thy1-YFP-H mouse was injected with reserpine (3~5 mg/kg I.P., dissolved in filtered 0.9% NaCl) for 5 days. Brain slices were prepared 2 hours after the last injection. For 6-OHDA experiments, each Thy1-YFP-H mouse was stereotaxically microinjected with 6-OHDA (2.5 mg/ml, 100 nl/min speed, 1 μl, dissolved in filtered 0.9% NaCl) targeting the medial forebrain bundle in the right hemisphere (AP: −0.9 mm, ML: −1.1 mm, DV: −4.8 mm). Brain slices were prepared for whole-cell recording 5~7 days after 6-OHDA injection. SCH23390 (0.25mg/kg i.p., twice daily), Haloperidol (3 mg/kg i.p., once daily) and Raclopride (0.4 mg/kg, i.p., twice daily) were used to block D1 and D2 receptors *in vivo*. Because Sulpiride does not pass through blood-brain barrier, Sulpiride was only used in *ex vivo* experiments.

De novo spine formation

De novo spine formation methods were described previously by Kwon et. al. [13]. Because dopamine is critically involved in initial synaptogenesis during the second postnatal week (postnatal day 7–14) *in vivo*[33], we performed our analysis in acute cortical brain slices from young animals (postnatal day 15–18). Thy1-eYFP-H mice were deeply anesthetized with isoflurane and decapitated. The brain was quickly removed and placed into chilled artificial cerebrospinal fluid (ACSF), and 300 μm coronal slices were prepared as described above. Slices were recorded within 4 hours after recovery and all recordings were performed at 33–34°C. Two-photon imaging and uncaging of MNI-caged glutamate was performed with a custom-built microscope equipped with two Ti:Sapphire lasers (Mai Tai, Spectra-Physics), as described previously[13]. Laser wavelengths were tuned to 925 nm and 720 nm for imaging of eYFP and glutamate uncaging, respectively. Slices were superfused with Mg^{2+}-free ACSF containing 5 mM MNI-caged glutamate. 2-photon imaging and glutamate uncaging were performed on apical oblique dendrites of layer V pyramidal neurons in primary motor cortex (M1). Uncaging laser power was tuned to ~50 mW at the back aperture of the objective (60×, NA 1.1, Olympus) to trigger glutamate uncaging. Uncaging position was chosen based on criteria described previously[13]. Briefly, the surface of the dendrite had to be smooth at the immediate vicinity of the uncaging spot, and there should be at least one spine presented within 5 μm of the uncaging spot to ensure the capability of the dendrite for spinogenesis. *De novo* spine formation was induced by 40 pulses (0.5 ms) of uncaging laser at 5 Hz at a spot approximately 0.5 μm away from the border of the selected dendrites. To test the efficacy of glutamate uncaging, whole-cell patch-clamp recording and two-photon Ca^{2+} imaging were simultaneously performed. For voltage-clamp recording, layer V pyramidal neurons were filled with internal solution containing 130 mM $CsCH_3SO_3$, 8 mM NaCl, 10 mM HEPES, 10 mM Na_2-Phosphocreatine, 0.4 mM Na_2GTP, 4 mM MgATP, 3 mM Na-Ascorbate, and 1.7 mM QX-314 (pH 7.2). For two-photon Ca^{2+} imaging, Alexa

Fluor-594 (25 μM) and Fluo-5F (300 μM) were add to the internal solution. Cells were filled with the dyes for at least 20 min before the start of recording. Imaging and uncaging lasers were tuned to 830 and 720 nm, respectively. Glutamate uncaging was performed in the same conditions as for *de novo* spine formation, but at the spine head to induce Ca^{2+} influx to test the efficacy of glutamate uncaging. Uncaging-induced EPSCs and Ca^{2+}-transients were recorded at −70 mV.

Motor skill training: Single-seed reaching task

The mouse single-seed reaching task protocol has been described previously [25]. Before training animals were food-restricted to maintain about 90% of free feeding weight. The training chamber was constructed as a transparent Plexiglas box. A vertical slit was made on the front wall of the box for individual mouse to reaching for millet seeds. The whole training included shaping phase and training phase. In the shaping phase mice would familiarize with the training chamber, task requirements and show their preferred limbs. A small pile of millet seeds were placed in front of the slit and mice could use both paws to reach for them. Shaping was finished when 20 reach attempts were achieved within 20 min, and 70% limb preference was established. Both control and MPTP-treated mice could finish shaping in 2–5 days. Surgery for implanting chronic cranial window above motor cortex was carried out after shaping. The side of implanting was selected according to limb preference demonstrated in shaping. For example, if the preferred limb was left the window was implanted above the right motor cortex and vice versa. Training phase started at least two weeks after surgery. Every training day consisted of one session of 30 trials with preferred limb or 20 min. Seeds were presented one by one in front of the slit. A `successful reach' was that in which the mouse used preferred limb, retrieved the seed and put it into its mouth smoothly. Otherwise it was considered unsuccessful or failed reach. Success rates were the percentages of successful reaches over total reach attempts. All shaping and training sessions were carried out during the same time of the day. The control mice were littermates that also underwent the food restriction and housed in standard mouse cages, with up to four mice per cage. Mice that experienced complications after chronic window implantation surgery were excluded from the study.

Statistical analysis

Statistical analysis for long-term plasticity (LTP and LTD) among two or more groups was performed by comparing the average amplitude of responses over a 5-min period (25~30 min after induction protocol). Statistical significance of data was determined using non-parametric Mann-Whitney Rank Sum test and one-way ANOVA, followed by the appropriate post hoc test. For comparing the probability of *de novo* spine formation across conditions, Fisher's exact test was used. For comparing food pellet reaching behavior performance, 2-way ANOVA repeated measure was used.

All reagents were purchased from Sigma-Aldrich except R-CPP, Sulpiride, Picrotoxin, Raclopride and MNI-glutamate (from Tocris).

Supplementary Material

Refer to Web version on PubMed Central for supplementary material.

Acknowledgements

The authors thank Drs. Helen Bronte-Stewart, Lu Chen, and members of Ding laboratory for helpful discussions. Supported by grants from the NINDS/NIH NS075136 and NS091144 (J.B.D.), the Klingenstein Foundation (J.B.D.) and the National Natural Science Foundation of China No. 91132726, 91232306 (T.X.), Science Fund for Creative Research Groups of the National Natural Science Foundation of China No. 61421064, the Fundamental Research Funds for the Central Universities', HUST: 2014XJGH004 (T.X.) and the Director Fund of WNLO. We also thank WNLO-HUST Optical Bioimaging Core Facility for assistance with data acquisition.

Reference

1. Wichmann T, DeLong MR. Functional and pathophysiological models of the basal ganglia. Curr Opin Neurobiol. 1996; 6:751–758. [PubMed: 9000030]
2. Hosp JA, Pekanovic A, Rioult-Pedotti MS, Luft AR. Dopaminergic projections from midbrain to primary motor cortex mediate motor skill learning. The Journal of neuroscience : the official journal of the Society for Neuroscience. 2011; 31:2481–2487. [PubMed: 21325515]
3. Dawson TM, Barone P, Sidhu A, Wamsley JK, Chase TN. Quantitative autoradiographic localization of D-1 dopamine receptors in the rat brain: use of the iodinated ligand [125I]SCH 23982. Neurosci Lett. 1986; 68:261–266. [PubMed: 2944035]
4. Lidow MS, Goldman-Rakic PS, Rakic P, Innis RB. Dopamine D2 receptors in the cerebral cortex: distribution and pharmacological characterization with [3H]raclopride. Proceedings of the National Academy of Sciences of the United States of America. 1989; 86:6412–6416. [PubMed: 2548214]
5. Seamans JK, Yang CR. The principal features and mechanisms of dopamine modulation in the prefrontal cortex. Prog Neurobiol. 2004; 74:1–58. [PubMed: 15381316]
6. Descarries L, Lemay B, Doucet G, Berger B. Regional and laminar density of the dopamine innervation in adult rat cerebral cortex. Neuroscience. 1987; 21:807–824. [PubMed: 3627435]
7. Lewis DA, Campbell MJ, Foote SL, Goldstein M, Morrison JH. The distribution of tyrosine hydroxylase-immunoreactive fibers in primate neocortex is widespread but regionally specific. The Journal of neuroscience : the official journal of the Society for Neuroscience. 1987; 7:279–290. [PubMed: 2879896]
8. Kunori N, Kajiwara R, Takashima I. Voltage-sensitive dye imaging of primary motor cortex activity produced by ventral tegmental area stimulation. The Journal of neuroscience : the official journal of the Society for Neuroscience. 2014; 34:8894–8903. [PubMed: 24966388]
9. Molina-Luna K, et al. Dopamine in motor cortex is necessary for skill learning and synaptic plasticity. PloS one. 2009; 4:e7082. [PubMed: 19759902]
10. Braak H, et al. Staging of brain pathology related to sporadic Parkinson's disease. Neurobiol Aging. 2003; 24:197–211. [PubMed: 12498954]
11. Yuste R, Bonhoeffer T. Morphological changes in dendritic spines associated with long-term synaptic plasticity. Annu Rev Neurosci. 2001; 24:1071–1089. [PubMed: 11520928]
12. Engert F, Bonhoeffer T. Dendritic spine changes associated with hippocampal long-term synaptic plasticity. Nature. 1999; 399:66–70. [PubMed: 10331391]
13. Kwon HB, Sabatini BL. Glutamate induces de novo growth of functional spines in developing cortex. Nature. 2011; 474:100–104. [PubMed: 21552280]
14. Harvey CD, Svoboda K. Locally dynamic synaptic learning rules in pyramidal neuron dendrites. Nature. 2007; 450:1195–1200. [PubMed: 18097401]
15. Wiegert JS, Oertner TG. Long-term depression triggers the selective elimination of weakly integrated synapses. Proceedings of the National Academy of Sciences of the United States of America. 2013; 110:E4510–4519. [PubMed: 24191047]
16. Hayama T, et al. GABA promotes the competitive selection of dendritic spines by controlling local Ca2+ signaling. Nature neuroscience. 2013; 16:1409–1416. [PubMed: 23974706]

17. Harms KJ, Rioult-Pedotti MS, Carter DR, Dunaevsky A. Transient spine expansion and learning-induced plasticity in layer 1 primary motor cortex. The Journal of neuroscience : the official journal of the Society for Neuroscience. 2008; 28:5686–5690. [PubMed: 18509029]
18. Rioult-Pedotti MS, Friedman D, Donoghue JP. Learning-induced LTP in neocortex. Science. 2000; 290:533–536. [PubMed: 11039938]
19. Xu T, et al. Rapid formation and selective stabilization of synapses for enduring motor memories. Nature. 2009; 462:915–919. [PubMed: 19946267]
20. Yang G, Pan F, Gan WB. Stably maintained dendritic spines are associated with lifelong memories. Nature. 2009; 462:920–924. [PubMed: 19946265]
21. Ueno T, et al. Morphological and electrophysiological changes in intratelencephalic-type pyramidal neurons in the motor cortex of a rat model of levodopa-induced dyskinesia. Neurobiology of disease. 2014; 64:142–149. [PubMed: 24398173]
22. Holtmaat A, Svoboda K. Experience-dependent structural synaptic plasticity in the mammalian brain. Nature reviews. Neuroscience. 2009; 10:647–658. [PubMed: 19693029]
23. Zuo Y, Yang G, Kwon E, Gan WB. Long-term sensory deprivation prevents dendritic spine loss in primary somatosensory cortex. Nature. 2005; 436:261–265. [PubMed: 16015331]
24. Tsai J, Grutzendler J, Duff K, Gan WB. Fibrillar amyloid deposition leads to local synaptic abnormalities and breakage of neuronal branches. Nature neuroscience. 2004; 7:1181–1183. [PubMed: 15475950]
25. Cruz-Martin A, Crespo M, Portera-Cailliau C. Delayed stabilization of dendritic spines in fragile X mice. The Journal of neuroscience : the official journal of the Society for Neuroscience. 2010; 30:7793–7803. [PubMed: 20534828]
26. Meredith GE, Totterdell S, Potashkin JA, Surmeier DJ. Modeling PD pathogenesis in mice: advantages of a chronic MPTP protocol. Parkinsonism & related disorders. 2008; 14(Suppl 2):S112–115. [PubMed: 18585085]
27. Surmeier DJ, Ding J, Day M, Wang Z, Shen W. D1 and D2 dopamine-receptor modulation of striatal glutamatergic signaling in striatal medium spiny neurons. Trends in neurosciences. 2007; 30:228–235. [PubMed: 17408758]
28. Fuxe K, Manger P, Genedani S, Agnati L. The nigrostriatal DA pathway and Parkinson's disease. J Neural Transm Suppl. 2006:71–83. [PubMed: 17017512]
29. Gerfen CR, Surmeier DJ. Modulation of striatal projection systems by dopamine. Annu Rev Neurosci. 2011; 34:441–466. [PubMed: 21469956]
30. Hill TC, Zito K. LTP-induced long-term stabilization of individual nascent dendritic spines. The Journal of neuroscience : the official journal of the Society for Neuroscience. 2013; 33:678–686. [PubMed: 23303946]
31. Clem RL, Celikel T, Barth AL. Ongoing in vivo experience triggers synaptic metaplasticity in the neocortex. Science. 2008; 319:101–104. [PubMed: 18174444]
32. Kirkwood A, Silva A, Bear MF. Age-dependent decrease of synaptic plasticity in the neocortex of alphaCaMKII mutant mice. Proceedings of the National Academy of Sciences of the United States of America. 1997; 94:3380–3383. [PubMed: 9096402]
33. Tang K, Low MJ, Grandy DK, Lovinger DM. Dopamine-dependent synaptic plasticity in striatum during in vivo development. Proceedings of the National Academy of Sciences of the United States of America. 2001; 98:1255–1260. [PubMed: 11158626]
34. Frith CD, Bloxham CA, Carpenter KN. Impairments in the learning and performance of a new manual skill in patients with Parkinson's disease. Journal of neurology, neurosurgery, and psychiatry. 1986; 49:661–668.
35. Graybiel AM. Neurotransmitters and neuromodulators in the basal ganglia. Trends in neurosciences. 1990; 13:244–254. [PubMed: 1695398]
36. Hosp JA, Molina-Luna K, Hertler B, Atiemo CO, Luft AR. Dopaminergic modulation of motor maps in rat motor cortex: an in vivo study. Neuroscience. 2009; 159:692–700. [PubMed: 19162136]
37. Alexander GE, Crutcher MD. Functional architecture of basal ganglia circuits: neural substrates of parallel processing. Trends in neurosciences. 1990; 13:266–271. [PubMed: 1695401]

38. Schultz W. Behavioral dopamine signals. Trends in neurosciences. 2007; 30:203–210. [PubMed: 17400301]
39. Snyder GL, et al. Regulation of phosphorylation of the GluR1 AMPA receptor in the neostriatum by dopamine and psychostimulants in vivo. The Journal of neuroscience : the official journal of the Society for Neuroscience. 2000; 20:4480–4488. [PubMed: 10844017]
40. Picconi B, et al. Loss of bidirectional striatal synaptic plasticity in L-DOPA-induced dyskinesia. Nature neuroscience. 2003; 6:501–506. [PubMed: 12665799]
41. Steiner P, et al. Destabilization of the postsynaptic density by PSD-95 serine 73 phosphorylation inhibits spine growth and synaptic plasticity. Neuron. 2008; 60:788–802. [PubMed: 19081375]
42. Moore RY, Whone AL, Brooks DJ. Extrastriatal monoamine neuron function in Parkinson's disease: an 18F-dopa PET study. Neurobiology of disease. 2008; 29:381–390. [PubMed: 18226536]
43. Goldberg JA, et al. Enhanced synchrony among primary motor cortex neurons in the 1-methyl-4-phenyl-1,2,3,6-tetrahydropyridine primate model of Parkinson's disease. The Journal of neuroscience : the official journal of the Society for Neuroscience. 2002; 22:4639–4653. [PubMed: 12040070]
44. Pasquereau B, Turner RS. Primary motor cortex of the parkinsonian monkey: differential effects on the spontaneous activity of pyramidal tract-type neurons. Cereb Cortex. 2011; 21:1362–1378. [PubMed: 21045003]
45. Li Q, et al. Therapeutic deep brain stimulation in Parkinsonian rats directly influences motor cortex. Neuron. 2012; 76:1030–1041. [PubMed: 23217750]
46. Gradinaru V, Mogri M, Thompson KR, Henderson JM, Deisseroth K. Optical deconstruction of parkinsonian neural circuitry. Science. 2009; 324:354–359. [PubMed: 19299587]
47. Feng G, et al. Imaging neuronal subsets in transgenic mice expressing multiple spectral variants of GFP. Neuron. 2000; 28:41–51. [PubMed: 11086982]
48. Yang G, Pan F, Parkhurst CN, Grutzendler J, Gan WB. Thinned-skull cranial window technique for long-term imaging of the cortex in live mice. Nature protocols. 2010; 5:201–208. [PubMed: 20134419]

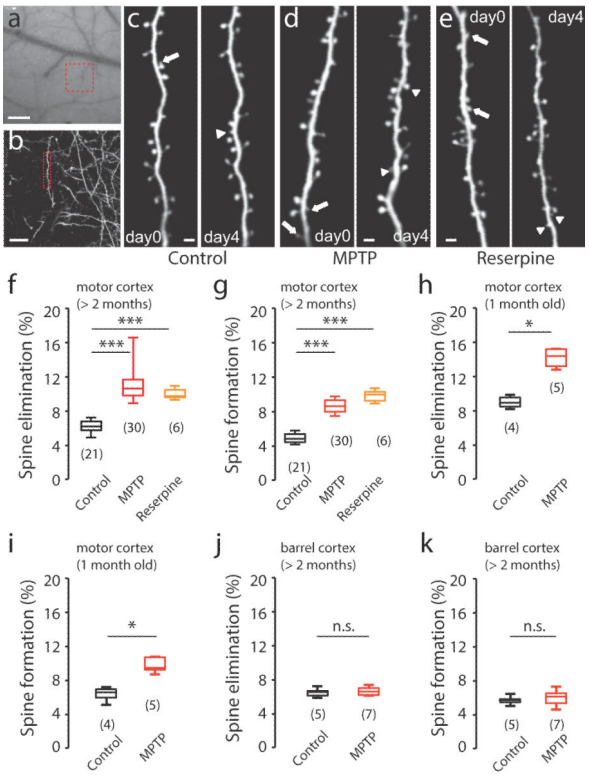

Figure 1. Spine turnover is increased in the dendritic spines of layer V pyramidal neurons of the motor cortex in two PD mouse models

(a) Motor cortex vasculature underneath the thinned skull of a Thy1-YFP-H control mouse. Red square indicates a region of interest (ROI), which is visualized and expanded in (b) to reveal layer V pyramidal neurons. (c–e) Repeated imaging of the same dendritic regions reveals spine elimination (arrows) and spine formation (arrowheads). Dendritic stretches from control, (c), which is expanded from (b), MPTP-treated, (d), and reserpine-treated, (e), mice. Images taken before (day0) or 4 days after (day4) drug injection. Scale bar represents 100 μm (a), 20 μm (b) or 2 μm (c–e). (f) Spine elimination in > 2 month old control, MPTP-injected, and reserpine-injected mice (Control: 6.2±0.1%, n=21; MPTP: 10.9±0.3%, n=30; P<0.0001; Reserpine: 10.0±0.3%, n=6; P=0.0003). (g) Spine formation in > 2 month old control, MPTP-injected and reserpine-injected mice (Control: 4.8±0.1%, n=21; MPTP: 8.5±0.2%; n=30; P<0.0001; Reserpine: 9.8±0.3%; n=6; P=0.0003, when compared to Control). (h) Spine elimination in 1 month old control and MPTP-injected mice (Control: 9.0±0.4%, n=4; MPTP: 14.2±0.5%, n=5; P=0.0159, Mann-Whitney). (i) Spine formation in 1 month old control and MPTP-injected mice (Control: 6.4±0.5%, n=4; MPTP: 9.8±0.4%; n=5; P=0.0159, Mann-Whitney). (j) Spine elimination in the barrel cortex of control and MPTP-injected mice (>2 months old) (Control: 6.5±0.2%, n=5; MPTP: 6.6±0.2%, n=7; P=0.6237, Mann-Whitney). (k) Spine formation in the barrel cortex of control and MPTP injected mice (> 2 months old) (Control: 5.6±0.2%, n=5; MPTP: 5.9±0.4%; n=7; P=0.5303, Mann-Whitney). Box-and-whisker plots indicate the minimum, 25th, 50th, 75th, and maximum percentiles. Data are presented as mean ± SEM The number in brackets indicates the number of animals used for analysis, *P < 0.05, ***P < 0.001, n.s.: non-significant, Mann-Whitney.

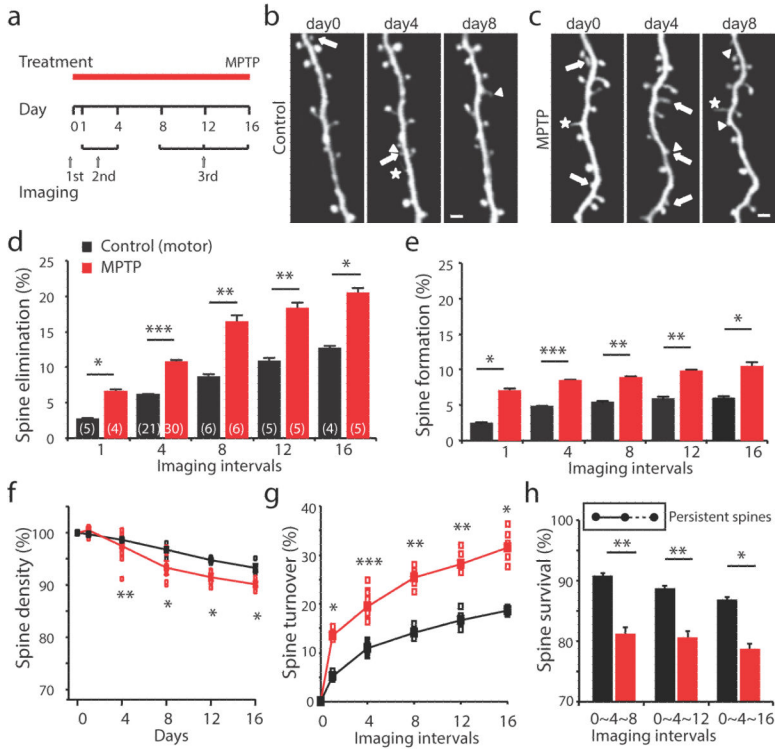

Figure 2. Spine dynamics in the motor cortex in PD mouse models

(a) Timeline of treatment and imaging. (b–c) Imaging at 0, 4, and 8 days in saline control (b) and MPTP-injected (c) mice. Arrows: spine eliminated, arrowheads: spine formed, and asterisks: filopodia. Scale bar represents 2 μm. (d–e) Spines eliminated (d) and formed (e) in the motor cortex of saline control and MPTP-treated mice over various time points (Spine elimination – Control: Day1, 2.7±0.2%, n=5; Day8, 8.6±0.4%, n=6; Day12, 10.9±0.5%, n=5; Day16, 12.7±0.4%, n=4; MPTP: Day1, 6.6±0.4%, n=4; Day8, 16.4±1.0%, n=6; Day12, 18.3±0.9%, n=5, Day16, 20.4±0.8%, n=5; P=0.0159 for Day1, P=0.0050 for Day8, P=0.0079 for Day12, P=0.0159 for Day 16; Spine formation – Control: Day1, 2.4±0.2%, n=5; Day8, 5.4±0.2%, n=6; Day12, 5.8±0.3%, n=5; Day16, 5.9±0.3%, n=4; MPTP: Day1, 7.0±0.4%; n=4; Day8, 8.9±0.2%, n=6; Day12, 9.8±0.2%, n=5, Day16, 10.4±0.6%, n=5, P=0.0159, for Day1, P=0.0022 for Day8, P=0.0079 for Day12, P=0.0195 for Day 16, Mann-Whitney). (f) Change of total spine density in the motor cortex in control and MPTP-treated mice. (day1, Control: 99.71±0.26%, n=5, MPTP: 100.40±0.52%, n=4, P=0.3252; day4, control: 98.64±0.13%, n=21, MPTP: 97.65±0.33%, n=30, P=0.0032; day8, control: 96.75±0.49%, n=6, MPTP: 92.45±0.88%, n=6, P=0.0411; day12, control: 94.98±0.28%, n=5, MPTP: 91.49±0.64%, n=5, P=0.0119; day16, control: 93.27±0.68%, n=4, MPTP: 89.99±0.33%, n=5, P=0.0159, Mann-Whitney). (g) Change of total spine turnover in the motor cortex in control and MPTP-treated mice (day1, control: 5.1±0.3%, n=5, MPTP: 13.6±0.5%, n=4, P=0.0195; day4, control: 11.0±0.2%, n=21, MPTP: 19.4±0.3%, n=30, P<0.0001; day8, control: 14.0±0.5%, n=6, MPTP: 25.3±1.1%, n=6, P=0.0022; day12, control: 16.7±0.8%, n=5, MPTP: 28.1±1.1%, n=5, P=0.0079; day16, control: 18.6±0.3%, n=4, MPTP: 30.9±1.4%, n=5, P=0.0159, Mann-Whitney). (h) Percentages of stable pre-existing spines in control and MPTP-treated mice (Control: day8, 90.8±0.3%, n=6; day12,

88.6±0.5%, n=5; day16, 86.8±0.4%, n=4; MPTP, day8, 81.2±0.9%, n=6; day12, 80.6±0.9%, n=5; day16, 78.7±0.8%, n=5; P=0.0050 for day8, P=0.0079 for day12, P=0.0159 for day 16, Mann-Whitney). Data are presented as mean ± SEM. Open boxes depict individual observations. The number in brackets indicates the number of animals used for analysis, *P< 0.05, **P < 0.01, ***P < 0.001, n.s.: non-significant, Mann-Whitney.

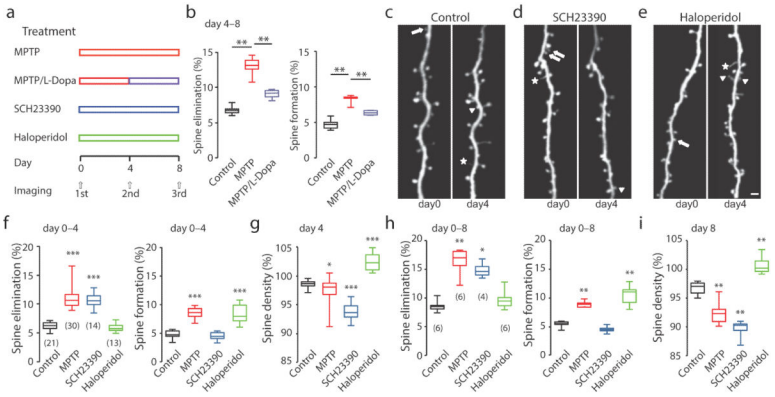

Figure 3. Spine elimination and formation are differentially regulated by different types of dopamine receptors in the motor cortex

(a) Timeline of treatment and imaging. (b) Spine elimination (left) and formation (right) over 4 days (day 4 – 8) in the motor cortex of saline control, MPTP-injected and MPTP/L-Dopa injected mice (Spine elimination – Control: 6.8±0.3%, n=6; MPTP: 13.0±0.5%, n=6, P=0.0022 compared to control; L-DOPA: 9.0±0.4%, n=4; P=0.0095 compared to MPTP; Spine formation – Control: 4.7±0.3%, n=6; MPTP: 8.3±0.3%, n=6, P=0.0050 compared to control; L-DOPA: 6.4±0.2%, n=4; P=0.0095 compared to MPTP; Mann-Whitney). (c–e) Repeated imaging of the same dendritic regions reveals spine elimination (arrows), spine formation (arrowheads) and filopodia (asterisks) in saline control (c), SCH23390-injected (d) and Haloperidol-injected (e) mice. Scale bar : 2 μm. (f) Spines eliminated (left) and formed (right) in the motor cortex of control, MPTP, SCH23390-injected and Haloperidol-injected mice (Spine elimination 0-4 days– control: 6.2±0.1%, n=21; SCH23390: 10.7±0.3%, n=14; P<0.0001 compared to control; Haloperidol: 5.9±0.2%, n=13; P=0.1956 compared to control; Spine formation 0-4 days– control: 4.8±0.1%, n=21; SCH23390: 4.5±0.2%, n=14; P=0.1475 compared to control; Haloperidol: 8.4±0.4%, n=13; P<0.0001 compared to control, Mann-Whitney). (g) Spine density of control, MPTP, SCH23390, and Haloperidol-injected mice at day 4 (Control: 98.64±0.13%, n=21; MPTP: 97.65±0.33%, n=30, P=0.0150 compared to control; SCH23390: 93.80±0.38%, n=14, P<0.0001 compared to control; Haloperidol: 102.53±0.44%, n=13, P<0.0001 compared to control). (h) Spines eliminated (left) and formed (right) in motor cortex of control, MPTP, SCH23390-injected and Haloperidol-injected mice (Spine elimination 0-8 days – control: 8.6±0.4%, n=6; MPTP: 16.4±1.0%, n=6, P=0.0050 compared to control; SCH23390: 14.9±0.7%, n=4, P=0.0139 compared to control; Haloperidol: 9.7±0.7%, n=6, P=0.3776 compared to control; Spine formation 0-8 days – control: 5.4±0.2%, n=6; MPTP: 8.9±0.2%, n=6, P=0.0022 compared to control; SCH23390: 4.5±0.3%, n=4, P=0.0871 compared to control; Haloperidol: 10.5±0.7%, n=6 P=0.0022 compared to control, Mann-Whitney). (i) Spine density of control, MPTP, SCH23390, and Haloperidol-injected mice at day 8 (Control: 96.75±0.49%, n=6; MPTP: 92.45±0.88%, n=6, P=0.0087 compared to control; SCH23390: 89.59±0.94% n=4, P=0.0095 compared to control; Haloperidol, 100.74±0.66%, n=6, P=0.0022 compared to control). Box-and-whisker plots indicate the minimum, 25th, 50th, 75th, and maximum percentiles. Data are presented as mean ± SEM. The number in brackets indicates the number of animal used for analysis, *P < 0.05, **P<0.01, ***P<0.001, comparing to control group, Mann-Whitney.

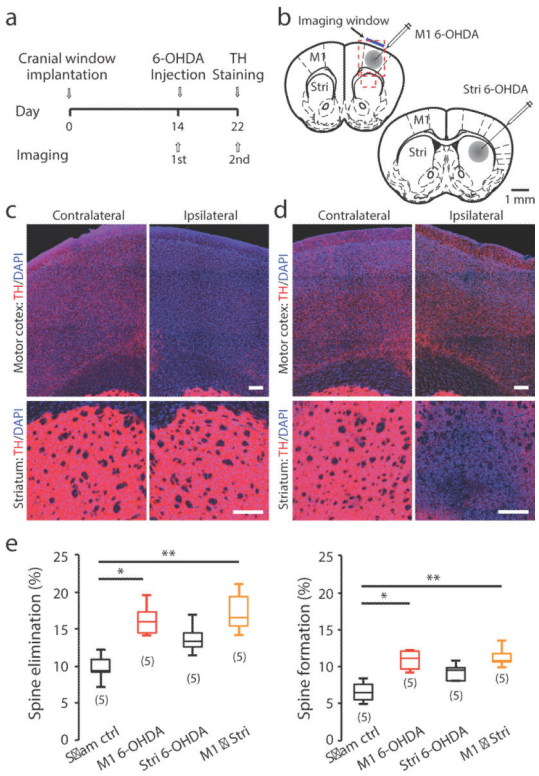

Figure 4. Spine elimination and formation are regulated by direct dopaminergic projection to M1

(a) Timeline of surgery and imaging. (b) Illustration of 6-OHDA injections into M1 and striatum. Injection needle was inserted lateral or posterior to the imaging window. (c–d) Representative images of M1 (upper) and dorsal lateral striatum (lower) demonstrating TH immunofluorescence in the contralateral and ipsilateral hemispheres in M1 (c) or striatum (d) 6-OHDA injected mice. Scale bars: 2 μm. (e) Spines eliminated (left) and formed (right) over 8 days in of sham control, M1 6OHDA, striatum 6-OHDA and M1 plus striatum 6-OHDA injected mice (Spine elimination – sham lesion control: 9.8±0.9%, n=5; M1 6-OHDA: 16.3±1.0%, n=5; striatum 6-OHDA: 13.7±0.9%, n=5; M1+striatum 6-OHDA: 17.3±1.3%, n=5) (Spine formation – sham lesion control: 6.6±0.6%, n=5; M1 6-OHDA: 10.9±0.6%, n=5; striatum 6-OHDA: 9.3±0.5%, n=5; M1+striatum 6-OHDA: 11.3±0.6%, n=5; P=0.0057, Kruskal-Wallis ANOVA, multiple comparisons). Box-and-whisker plots indicate the minimum, 25th, 50th, 75th, and maximum percentiles.

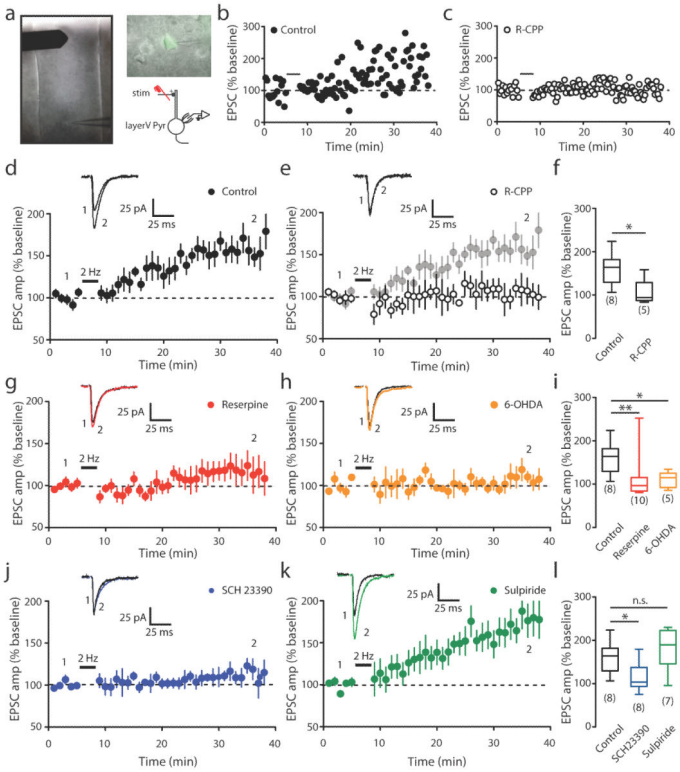

Figure 5. Long-term potentiation (LTP) is impaired following dopami ne depletion

(a) A sample image of a coronal slice showing the positions of stimulating and recording electrodes M1. Whole-cell patch clamp recording is performed in layer V pyramidal neuron (green). (b) Representative experiment illustrating LTP induction. (c) Representative experiment showing LTP induction in the presence of NMDA receptor blocker R-CPP (10 μM). (d–e) Summary data showing LTP inductions in control (d) and R-CPP (e) conditions. Average peak EPSC amplitude is shown over time (inset). (f) Average EPSC amplitude 25-30 min after LTP induction in control and R-CPP groups (LTP in control: 161.5% ±12.95%, n=8 cells from 6 mice; R-CPP: 105.3%±13.52%, n=5 cells from 3 mice, P=0.0186, Mann-Whitney). (g–h) Summary data showing LTP inductions in reserpine-injected (g) and 6-OHDA-lesioned (h) mice. (i) Average EPSC amplitude 25-30 min after LTP induction in control, reserpine-injected and 6-OHDA-lesioned mice (Reserpine: 112.8%±16.11%, n=10 cells from 5 mice, P=0.0085 compared to control; 6-OHDA: 109.9% ±8.28%, n=5 cells from 4 mice, P=0.0186 compared to control, Mann-Whitney). (j–k) Summary data showing LTP induction in the presence of D1 receptor antagonist SCH23390 (3 μM) (j) and D2 antagonist Sulpiride (5 μM) (k). (l) Average EPSC amplitude 25-30 min after LTP induction in control, SCH23390 and Sulpiride treated groups (SCH23390: 113.5% ±11.88%, n=8 cells from 5 mice, P=0.0207 compared to control; Sulpiride: 177.1%±18.21, n=7 from 4 mice, P=0.5358 compared to control, Mann-Whitney). Box-and-whisker plots indicate the minimum, 25th, 50th, 75th, and maximum percentiles. Data are presented as mean ± SEM. (Insert: average EPSCs before (1) and after (2) LTP induction. The numbers in brackets indicate the number of neurons recorded, *P< 0.05, **P< 0.01, n.s.: non-significant, Mann-Whitney).

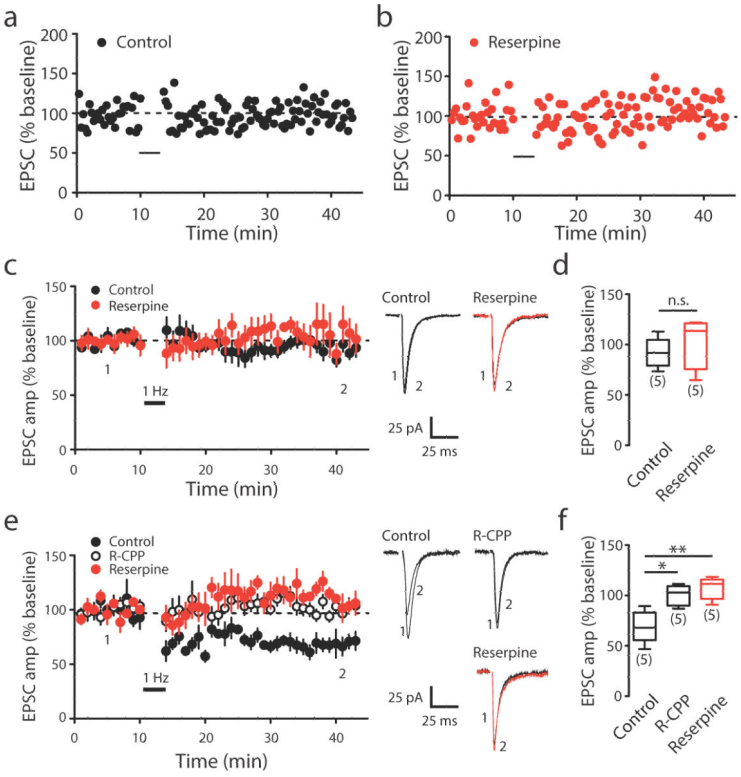

Figure 6. Long-term depression (LTD) following dopamine depletion

(a–b) Representative experiments showing LTD induction in control (a) and reserpine-injected (b) mice. (c) Summary data showing LTD induction in control and reserpine-injected mice. (d) Average EPSC amplitude 25-30 min after LTD induction in control and reserpine-injected mice (LTD in control: 91.9%±6.54%, n=5 cells from 3 mice; Reserpine: 103.4%±13.22%, n=5 cells from 5 mice, P=0.4127, Mann-Whitney). (e) Summary data showing LTD inductions in control, R-CPP-treated, and reserpine-injected conditions in young (3 weeks old) mice. (f) Average EPSC amplitude 25-30 min after LTD induction in control, R-CPP and reserpine groups. Black bar indicates LTD induction (control: 69.1% ±7.04%, n=5 cells from 3 mice; R-CPP: 100.2%±4.52%, n=5 cells from 3 mice, P=0.0159 compared to control; Reserpine: 107.3%±4.86%, n=5 cells from 3 mice, P=0.0079 compared to control, Mann-Whitney). Box-and-whisker plots indicate the minimum, 25th, 50th, 75th, and maximum percentiles. Data are presented as mean ± SEM. The number in brackets indicates the number of neurons recorded, *P<0.05, **P<0.01, n.s.: non-significant, comparing to control group, Mann-Whitney. Inserts: average EPSCs before (1) and after (2) LTD induction.

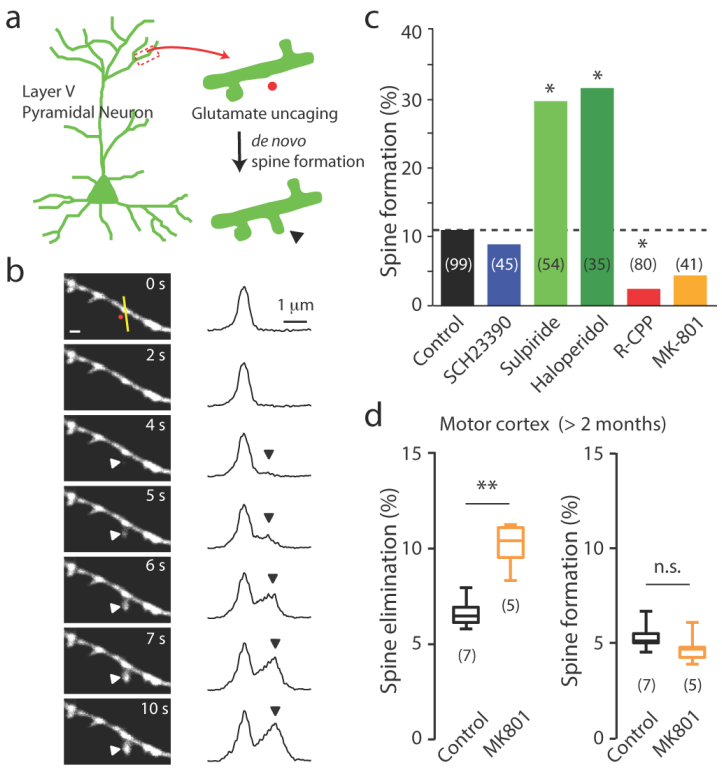

Figure 7. Spine formation and elimination are separately regulated

(a) Schematic showing *de novo* spine formation (arrow head) using combined 2-photon imaging and 2-photon glutamate uncaging (red circle). (b) Time-lapse images show *de novo* spine formation induced by photolytic glutamate release (left). Fluorescence intensity profiles along the yellow line showing increase of spine head fluorescence (arrowhead) (right). (c) Summary statistics for *de novo* spine formation in various conditions. The dotted line indicates the percentage of successful spine formation in the control condition. The number in brackets indicates the number of induction attempts for each condition (SCH23390: 8.9%, n=45, P=1, Fisher's exact test; Sulpiride: 29.6%, n=54, P = 0.0049, Fisher's exact test; Haloperidol: 31.43%, n=35, P=0.0083, Fisher's exact test; R-CPP: 2.5%, n=80, P=0.0302, Fisher's exact test; MK801: 4.9%, n=41, P=0.3624, Fisher's exact test, all compared to control group). (d) Spines eliminated (left) and formed (right) over 4 days in control and MK801-treated mice (Spine elimination – control: 6.6±0.3%, n=7, MK801: 10.1±0.5%, n=5; P=0.0025 compared to control; Spine formation – control: 5.3±0.3%, n=7, MK801: 4.7±0.4%, n=5; P=0.1490 compared to control, Mann-Whitney). Box-and-whisker plots indicate the minimum, 25th, 50th, 75th, and maximum percentiles. Data are presented as mean ± SEM. **P<0.01, n.s.: non-significant, Mann-Whitney.

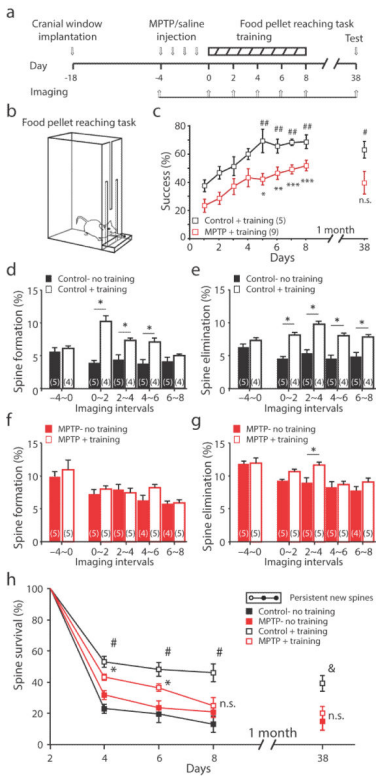

Figure 8. Dopamine depletion impairs motor skill learning and learning-induced spine formation and elimination

(a) Timeline of experiments. (b) Illustration of the food pellet reaching motor training. (c) Average success rates during training for control and MPTP-injected mice (day 1, control: 37.52±4.27%, MPTP: 23.33±4.61%; day 38, control: 63.06±5.89%, P<0.05 compared to control day1, MPTP: 39.61±8.05%, P>0.05 compared to MPTP day1, repeated measure 2-way ANOVA with post-hoc comparisons). (#P < 0.05, ##P<0.01, compared to day 1 control; *P < 0.05, **P<0.01, ***P<0.001, n.s.: non-significant, compared to day 1 MPTP-injected mice). (d–e) Spines formed (d) and eliminated (e) in control mice during motor skill learning (Spine formation – 0~2: control no training 3.93±0.41%, n=5, control + training 10.22±0.82%, n=4, P=0.0159; 2~4: control no training 4.40±0.80%, n=5, control + training 7.28±0.45%, n=4, P=0.0317; 4~6: control no training 3.85±0.61%, n=5, control + training 7.10±0.65%, n=4, P=0.0317; 6~8: control no training 4.23±0.59%, n=5, control + training 5.06±0.20%, n=4, P=0.3252; Spine elimination – 0~2: control no training 4.61±0.30%, n=5, control + training 8.13±0.45%, n=4, P=0.0159; 2~4: control no training 5.43±0.54%, n=5, control + training 9.76±0.50%, n=4, P=0.0159; 4~6: control no training 4.62±0.51%, n=5, control + training 8.06±0.39%, n=4, P=0.0195; 6~8: control no training 4.91±0.65%, n=5, control + training 7.83±0.39%, n=4, P=0.0159, Mann-Whitney). (f–g) Spines formed (f) and eliminated (g) in MPTP-treated mice during motor skill learning (Spine formation – 0~2: MPTP no training 7.22±0.22%, n=5, MPTP + training 8.01±0.34%, n=5, P=0.1508; 2~4: MPTP no training 7.95±0.75%, n=5, MPTP + training 7.45±0.59%, n=5, P=0.6905, 4~6: MPTP no training 6.24±0.49%, n=4, MPTP + training 8.24±0.50%, n=5; P=0.1111, 6~8: MPTP no training 5.79±0.59%, n=4, MPTP + training 5.90±0.58%, n=5, P=0.9048; Spine elimination – 0~2: MPTP no training: 9.24±0.67%, n=5, MPTP + training 10.67±0.53%,

n=5, P=0.1425; 2~4: MPTP no training 8.96±0.80%, n=5, MPTP + training 11.58±0.66%, n=5, P=0.0317, 4~6: MPTP no training 8.26±0.86%, n=4, MPTP + training 8.66±0.44%, n=5, P=0.9048, 6~8: MPTP no training 7.78±0.35%, n=4, MPTP + training 9.11±0.44%, n=5, P=0.1111, Mann-Whitney). (h) New spines which formed during the initial 2-day training that remained, as a function of time, for control, trained, MPTP-injected, and trained MPTP-injected mice (Control no training: day4, 23.00±2.91%; day6, 19.67±5.49%; day8, 13.00±5.39%; Control + training: day4, 53.14±3.48%; day6, 48.28±4.49%; day8, 46.19±5.81%; day38, 39.22±4.93%; P=0.0159 for day4, day6, day 8 respectively; MPTP no training: day4, 31.83±2.91%; MPTP + training: day4, 43.28±2.15%, P=0.0238; MPTP no training: day6, 23.61±4.61%, MPTP + training: day6 36.56±2.42%, P=0.0397; MPTP no training: day 8, 20.83±3.31%, MPTP + training: day 8, 24.83±5.32%, P=0.9683; MPTP no training: day 38, 14.93±5.65%, MPTP + training: day 38, 20.39±4.11%, P=0.7381; Mann-Whitney). Data are presented as mean ± SEM. *P<0.05, n.s.: non-significant, compared to MPTP-injected non trained mice; #P<0.05, compared to control non trained mice; & P<0.05, compared to trained MPTP-injected mice, Mann-Whitney.